OXYGEN ISOTOPIC COMPOSITIONS OF CHONDRULES FROM THE PRIMITIVE CV3 CHONDRITE RBT 04143. H. Ishida[1], S. Itoh[2], H. Yurimoto[3], T. Nakamura[1]. [1]Department of Earth and Planetary Material Sciences, Tohoku University, Aoba-ku, Sendai, Japan (h-ishida@s.tohoku.ac.jp), [2]Department of Earth and Planetary Sciences, Kyoto University, Sakyou-ku, Kyoto, Japan, [3]Natural History Science, Hokkaido University, Kita-ku, Sapporo, Japan.

Introduction: Chondrules are spherical igneous silicates that formed by the flash heating episodes in the protoplanetary disk. The mineralogical and oxygen isotopic compositions of chondrules constrain the physicochemical conditions of chondrule forming environments. The CV3 carbonaceous chondrites are classified into three subtypes: oxidized Allende-like ($CV3_{OxA}$), oxidized Bali-like ($CV3_{OxB}$), and reduced ($CV3_{Red}$) based on several criteria [1,2]. The $CV3_{Red}$ chondrites are known as the most primitive chondrite in CV3s, because they have undergone the least degrees of aqueous alteration and thermal metamorphism [3-6]. Roberts Massif (RBT) 04143 is classified as a $CV3_{Red}$ chondrite [7]. In this study, we obtained new mineralogical and oxygen isotopic data of chondrules from the primitive CV3 carbonaceous chondrite RBT 04143. Oxygen isotope measurements were performed at Hokkaido University using the Cameca ims-1270 SIMS.

Results and Discussion: RBT 04143 has rounded undeformed chondrules and a very porous matrix. The Fe-Mg zoning at the periphery of chondrules is largely absent, indicating that chondrules have not experienced intensive thermal metamorphism on the parent asteroid. Major opaque phases are kamacite, taenite, pyrrhotite and troilite. Magnetite is a minor phase. Secondary minerals such as nepheline and sodalite are absent or rare. This suggests that RBT 04143 has escaped Fe-alkali-metasomatic alteration that occurred in many other CV3 chondrites. We selected 14 chondrules for oxygen isotope analysis based on chondrule types and grain size of anorthite which will be analysed for future aluminium-magnesium dating. The selected chondrules include nine Type-I chondrules (Mg#≧90 for olivine and low-Ca pyroxene), three Type-II chondrules (Mg#<90), and two plagioclase-rich chondrules (Fig. 1). The oxygen isotope compositions of all chondrules distributed along a slope ~1 line that is a typical CV3 compositional field in the oxygen three-isotope diagram [e.g.,8].

Type-I chondrules (porphyritic and barred olivine chondrule); The oxygen isotope compositions of eight Type-I porphyritic chondrules and one barred olivine (BO) chondrule were measured. The results of the oxygen isotope ratios in 5 out of 9 Type-I chondrules including BO (Mg# of the 5 chondrules ranges from 96 to 99) indicate that most of $\delta^{18}O$ values distribute lower than -6 ‰ down to -12 ‰. On the other hand, in the other 4 chondrules (Mg# ranges from 95 to 98), multiple minerals are distributed between -1 and -8 ‰ in $\delta^{18}O$. Four Type-I chondrules contain plagioclase with An# from 80 to 99. Two Type-I chondrules contain mesostasis glass. These plagioclase and glass are larger than 10μm in diameter and almost free of secondary alteration effects. Plagioclase in one chondrule and mesostasis glass in one chondrule show oxygen compositions similar to co-existing olivine and pyroxene (e.g., Figs. 2A,C), but plagioclase in three chondrules and glass in one chondrule has ^{16}O-poor compositions relative to coexisting mafic minerals, ranging from 0 to 8 ‰ in $\delta^{18}O$.

Plagioclase-rich chondrules; We measured oxygen isotope ratios of two plagioclase-rich chondrules that consist of plagioclase, low-Ca pyroxene, high-Ca pyroxene, and olivine. The average Mg# for olivine and low-Ca pyroxene in one chondrule is 96, while that for low-Ca pyroxene in the other chondrule is 98. $\delta^{18}O$ values of olivine and pyroxenes are lower than 0 ‰, whereas all plagioclase grains distribute more ^{16}O-poor areas in a range from 4 to 9 ‰ on $\delta^{18}O$.

Type-ⅡIchondrules; In Type-II chondrules (Mg# for olivine ranges from 62 to 75), most data distribute at more ^{16}O-poor field ($\delta^{18}O > 0$ ‰) compared to Type-I and plagioclase-rich chondrules. One out of 3 chondrules, the $\delta^{18}O$ values of olivine are lower than 0 ‰, while the plagioclase is plotted in a ^{16}O-poor area ($\delta^{18}O$ ~8‰).

The environment of CV3-chondrule forming regions and that of post heating episode; The average oxygen isotope compositions of chondrules show two different populations. This result indicates that chondrules from RBT 04143 formed from two types of oxygen isotope reservers and accreted to the parent asteroid in a CV3 chondrite accretionary region in the protoplanetary disk.

After formation, many chondrules seem to have been reheated in the disk, because mesostasis glass and plagioclase crystals in many chondrules in RBT 04143 show various ^{16}O-poor compositions ranging from 0 to 10 ‰ in $\delta^{18}O$. The ^{16}O-poor composition can be explained either by reheating in the nebula or by thermal alteration in the parent asteroid. Small olivine crystals in the matrix of RBT 04143 retain a wide Fe/Mg variation [7], suggesting that thermal effect in the parent asteroid of RBT 04143 is limited. In addition, evidence of secondary hydrous alteration is absent in this meteorite [7]. Therefore, we suppose that the ^{16}O-poor

compositions of plagioclase and glass are established in the nebula after formation of chondrules.

In one plagioclase-rich chondrule, a wide area in the interior of the chondrule is composed of high-Ca pyroxene and anothitic plagioclase (Fig. 2B). The mineralogy suggests that the two minerals formed together during cooling in the chondrule formation event. However, oxygen isotope ratios of the two minerals are different: plagioclases show ^{16}O-poor compositions from 4 to 9 ‰ in δ^{18}O, while high-Ca pyroxene shows ^{16}O-poor composition (δ^{18}O ~−1‰), similar to coexisting olivine (Fig. 2D). Since plagioclase and high-Ca pyroxene formed together in the chondrule formation event, the difference in oxygen composition cannot be ascribed to chondrule formation event. The difference must have established at reheating event. But if reheating occurred at high temperature, the two minerals melted together because of the eutectic composition. In this case, oxygen exchange occurred between nebular gas and plagioclase+pyroxene melt, resulting in formation of ^{16}O-poor plagioclase and high-Ca pyroxene. To make ^{16}O-poor plagioclase and ^{16}O-rich high-Ca pyroxene in one chondrule, the reheating must have occurred at the subsolidus temperature. During reheating period, both plagioclase and high-Ca pyroxene were not melted, but only plagioclase could exchanged oxygens with nebular gas because of higher oxygen diffusion rates than high-Ca pyroxene [9,10].

In fact, the ^{16}O-poor compositions (0 to 10 ‰ on δ^{18}O) of plagioclase and mesostasis glass are similar to oxygen compositions of melilite in CAIs in this meteorite and other CV3 chondrites [e.g., 11]. The ^{16}O-poor compositions of the CAI melilite was established by oxygen exchange between nebulsar gas and CAIs at subsolidus temperature during reheating events [12]. Therefore, the ^{16}O-poor compositions of plagioclase and mesostasis glass found in primitive CV3 RBT 04143 may suggest that the reheating events experienced by CAIs also heated chondrules and changed their oxygen compositions.

Acknowledgement: RBT 04143 was allocated to us from NASA/JSC. This work was supported by a Research Fellowship for Young Scientists from the Japan Society for the Promotion of Science (No. 24-5780)

References: [1] McSween Jr., H.Y. (1977) *GCA 41*, 1777-1790. [2] Weisberg M.K. et al. (1997) *Met. Planet. Sci., 32*, A138-139. [3] Krot A.N. et al. (1995) *Met. Planet. Sci., 30*, 748-775. [4] Krot A.N. et al. (1998a) *Met. Planet. Sci., 33*, 1065-1085. [5] Krot A.N. et al. (1998b) *Met. Planet. Sci., 33*, 623-645. [6] Krot A.N. et al. (2004) *Antarc. Meteorite. Res., 17*, 153-171. [7] Ishida H. et al. (2012) *Polar. Sci., 6*, 252-262. [8] Clayton R.N. (1993) *Ann. Rev. Earth Planet, Sci 21*, 115-149. [9] Ingrin J. et al. (2001) *Earth Planet. Sci. Lett, 192*, 347-361. [10] Ryerson F. J. and McKeegan K. D. (1993) *GCA 58*, 3713-3734. [11] Scott E. R. D. and Krot A. N. (2003) *Comets and Planets*, Vol. 1 (ed.A.M. Davis) *Treatise on Geochemistry* (eds. H.D. Holland and K.K. Turekian), Elsevier, Oxford, pp. 143-200. [12] Fagan, T. J. et al. (2004) *Met. Planet. Sci. 39*, 1257-1272.

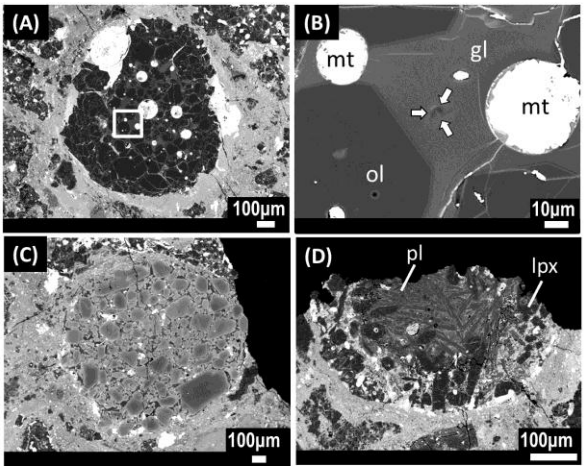

Fig. 1. Back-scattered electron images of chondrules. (A) Type-I porphyritic chondrule. (B) The enlarged image of glass in Type-I chondrule, shown as a box in (A). SIMS measurement spot is indicated by arrows. (C) Type-II porphyritic chondrule. (D) Plagioclase-rich chondrule. ol=olivine, mt=metal, gl=glass, pl=plagioclase, lpx= low-Ca pyroxene.

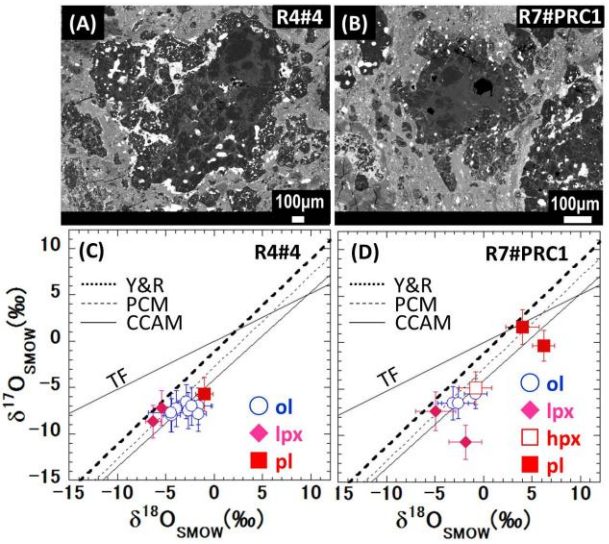

Fig. 2. Back scattered electron images and oxygen three-isotope diagrams of Type-I porphyritic chondrule R4#4(A, C) and plagioclase-rich chondrule R7#PRC1 (B, D). ol=olivine, lpx=low-Ca pyroxene, hpx=high-Ca pyroxene, pl=plagioclase.